bioRxiv preprint doi: https://doi.org/10.1101/337790; this version posted June 3, 2018. The copyright holder for this preprint (which was not certified by peer review) is the author/funder, who has granted bioRxiv a license to display the preprint in perpetuity. It is made available under aCC-BY 4.0 International license.

1 # Dynamic decoupling of biomass and lipid biosynthesis by

2 # autonomously regulated switch

3 short title: Dynamic decoupling of biomass and lipid synthesis

4

5 Suvi Santala[1]*, Elena Efimova[1], Ville Santala[1]

6

7 [1]Laboratory of Chemistry and Bioengineering, Tampere University of Technology,

8 Korkeakoulunkatu 8, FI-33720, Tampere, Finland

9

10 *Corresponding author

11

12 Email addresses:

13 SS: suvi.santala@tut.fi

14 EE: elena.efimova@tut.fi

15 VS: ville.santala@tut.fi

16

17

bioRxiv preprint doi: https://doi.org/10.1101/337790; this version posted June 3, 2018. The copyright holder for this preprint (which was not certified by peer review) is the author/funder, who has granted bioRxiv a license to display the preprint in perpetuity. It is made available under aCC-BY 4.0 International license.

18 ## Abstract

19 For improving the microbial production of fuels and chemicals, gene knock-outs and
20 overexpression are routinely applied to intensify the carbon flow from substrate to
21 product. However, their possibilities in dynamic control of the flux between the
22 biomass and product synthesis are limited, whereas dynamic metabolic switches can
23 be used for optimizing the distribution of carbon and resources. The production of
24 single cell oils is especially challenging, as the synthesis is strongly regulated, competes
25 directly with biomass, and requires defined conditions, such as nitrogen limitation.
26 Here, we engineered a metabolic switch for redirecting carbon flow from biomass to
27 wax ester production in *Acinetobacter baylyi* ADP1 using acetate as a carbon source.
28 Isocitrate lyase, an essential enzyme for growth on acetate, was expressed under an
29 arabinose inducible promoter. The autonomous downregulation of the expression is
30 based on the gradual oxidation of the arabinose inducer by a glucose dehydrogenase
31 *gcd*. The depletion of the inducer, occurring simultaneously to acetate consumption,
32 switches the cells from a biomass mode to a lipid synthesis mode, enabling the
33 efficient channelling of carbon to wax esters in a simple batch culture. In the
34 engineered strain, the yield and titer of wax esters were improved by 3.8 and 3.1 folds,
35 respectively, over the control strain. In addition, the engineered strain accumulated
36 wax esters 19% of cell dry weight, being the highest reported among microbes. The
37 study provides important insights into the dynamic engineering of the biomass-
38 dependent synthesis pathways for the improved production of biocompounds from
39 low-cost, sustainable substrates.

bioRxiv preprint doi: https://doi.org/10.1101/337790; this version posted June 3, 2018. The copyright holder for this preprint (which was not certified by peer review) is the author/funder, who has granted bioRxiv a license to display the preprint in perpetuity. It is made available under aCC-BY 4.0 International license.

40 ## Keywords

41 Lipid biosynthesis, wax esters, acetate, dynamic control, decoupling, autonomous
42 circuit

43 ## Significance statement

44 In the biological production, one of the greatest challenges is to find ways for optimal
45 distribution of resources between cell growth, maintenance, and product synthesis.
46 Robust and reliable circuits are required to allow autonomous switching of cells from
47 biomass mode to lipid synthesis mode. Dynamic production of single cell oils such as
48 triacylglycerols and wax esters is especially challenging due to the strong regulation.
49 We present a dynamic genetic circuit based on conditional knockdown of a glyoxylate
50 shunt enzyme, which is essential for cell growth. By gradual repression of the gene,
51 the cells autonomously switch from biomass mode to product synthesis mode. We
52 demonstrate the functionality of the circuit by using bacterium *Acinetobacter baylyi*
53 ADP1 for the production of long chain alkyl esters, namely wax esters, with titer and
54 yield improved by over 3-fold using acetate as the carbon source.

55 ## Abbreviations

56 WE – wax esters, AceA – isocitrate lyase

57 ## 1. Background

58 Metabolic engineering and synthetic biology provide powerful means for the bio-
59 based production of a variety of chemicals and other commodities by engineered
60 microbes. Compared to conventional chemical synthesis, the superiority of biological
61 production systems lies in the possibility to synthesize both the catalyst (i.e. the cell

bioRxiv preprint doi: https://doi.org/10.1101/337790; this version posted June 3, 2018. The copyright holder for this preprint (which was not certified by peer review) is the author/funder, who has granted bioRxiv a license to display the preprint in perpetuity. It is made available under aCC-BY 4.0 International license.

62 factory) and the product itself from very simple chemical compounds, such as sugars
63 or organic acids. However, the challenge is to develop a system, which optimally
64 distributes the resources and carbon flux between building up the catalyst and
65 operating the catalyst for the actual production; extensive cell growth takes resources
66 from the product synthesis, whereas too excessive flux towards product synthesis may
67 result in reduced growth, insufficient cofactor regeneration, low enzyme expression
68 levels, and eventually poor titers. To address the challenges related to the optimal
69 distribution of cellular resources, a number of dynamic circuit designs targeting the
70 central pathway nodes have been recently developed (1). While growth-associated
71 genes responsible for central carbon metabolism cannot be directly deleted, various
72 strategies for decoupling growth and product synthesis have been introduced; Soma
73 et al. constructed a metabolic toggle switch for conditional knockout of citrate
74 synthase *gltA,* an enzyme required for functional tricarboxylic acid (TCA) cycle (2). The
75 switch allowed an induced shift of carbon flow from TCA cycle to synthetic isopropanol
76 pathway. More recently, the system was further improved by introducing a sensor-
77 regulator system responsive to a defined cell density (3). Solomon et al. introduced a
78 dynamic approach to controlling the glycolytic flux; antisense RNA technology and an
79 inverting gene circuit were employed for inhibiting the activity of glucokinase (Glk),
80 resulting in a controlled growth rate and a reduced production of acetate (4).
81 Brockman and Prather introduced another example of a dynamic regulation system,
82 where they developed a circuit for dynamic knockdown of phosphofructokinase-1
83 (Pfk-1), the enzyme responsible for the key step in the glycolytic pathway regulating
84 glucose-6-phosphate flux. By the temporal control of Pfk-1 degradation, glucose-6-

bioRxiv preprint doi: https://doi.org/10.1101/337790; this version posted June 3, 2018. The copyright holder for this preprint (which was not certified by peer review) is the author/funder, who has granted bioRxiv a license to display the preprint in perpetuity. It is made available under aCC-BY 4.0 International license.

85 phosphate could be efficiently directed to heterologous *myo*-inositol synthesis
86 pathway instead of biomass production (5). In a previous work, Doong et al. further
87 improved the system with a *myo*-inositol responsive dynamic sensor that regulated
88 the downstream enzymes of the pathway in converting *myo*-inositol to glucarate. The
89 introduced systems represent highly elegant examples of advanced metabolic control,
90 but the complex circuit designs can be prone to destabilization in prolonged
91 cultivations and function unexpectedly in scaled-up processes (6). Thus, reliable
92 metabolic control systems with simple and robust operation would be also desired.
93
94 Microbial storage compounds, such as polyhydroxyalkanoates (PHA), triacylglycerols
95 (TAG) and wax esters (WE), are industrially relevant and desirable molecules due to
96 their vegetable oil like properties and broad applicability in e.g. fuel, nutritional,
97 cosmetic, and pharmaceutical industries. However, the production of the long carbon
98 chain products derived from fatty acyl-CoA requires significant energy investments
99 from the cell. In addition, the synthesis of storage compounds directly competes with
100 biomass production and is strongly regulated, growth-phase dependent, and requires
101 high amounts of cofactors and excess carbon along with limitation on other nutrients,
102 such as nitrogen (7, 8). While strategies for dynamically regulated production of free
103 fatty acids (FFA) and FA derived products have been introduced (9, 10), means for
104 overcoming the challenges of storage lipid synthesis regulation are still lacking.
105 Therefore, the production processes are conventionally improved by non-specific
106 means, such as bioprocess optimization or in conditions with a defined carbon-
107 nitrogen ratio (11). As an example of a more advanced approach, Xu et al. established

bioRxiv preprint doi: https://doi.org/10.1101/337790; this version posted June 3, 2018. The copyright holder for this preprint (which was not certified by peer review) is the author/funder, who has granted bioRxiv a license to display the preprint in perpetuity. It is made available under aCC-BY 4.0 International license.

108 a semi-continuous culture system with model-aided bioprocess optimization and cell
109 recycling, which allowed efficient TAG production and high productivities even with
110 dilute acetate feed (12). While also metabolic engineering strategies have been
111 employed for improving TAG (13-16) and WE synthesis (17, 18) in microbes, efficient
112 overproduction of acetyl-CoA coupled with dynamic resource distribution between
113 biomass and storage lipid synthesis remains a challenge.
114
115 When microbes are cultivated on non-glycolytic substrates, such as acetate or fatty
116 acids, complete TCA cycle yielding carbon dioxide cannot be utilized for anabolic
117 processes. In those circumstances, the cells have to rely on an alternative route,
118 namely glyoxylate cycle, which bypasses the two decarboxylation steps of TCA cycle.
119 The key enzyme in the glyoxylate cycle is isocitrate lyase (AceA), responsible for
120 converting isocitrate to glyoxylate and succinate. It was previously demonstrated that
121 a knock-out of the isocitrate lyase in *Pseudomonas putida* improved the production of
122 PHAs when grown on gluconate, apparently for providing surplus acetyl-CoA for the
123 PHA synthesis (19). Some bacteria also exhibit an alternative pathway for glycolysis,
124 such as the modified Entner-Doudoroff pathway of certain *Acinetobacter* strains (20,
125 21). An interesting feature of the glycolysis of *Acinetobacter* is the oxidation of glucose
126 to gluconate prior the transport to cells. In the absence of glucose, the first enzyme of
127 the pathway, glucose dehydrogenase Gcd, can unselectively oxidize other sugar
128 compounds present in the medium, such as pentoses, without the capability to utilize
129 them as a carbon source (22-24). Importantly, this feature does not interfere with the
130 utilization of non-glycolytic carbon sources, such as organic acids, and can be

bioRxiv preprint doi: https://doi.org/10.1101/337790; this version posted June 3, 2018. The copyright holder for this preprint (which was not certified by peer review) is the author/funder, who has granted bioRxiv a license to display the preprint in perpetuity. It is made available under aCC-BY 4.0 International license.

131 considered being 'orthogonal' to the substrate utilization. Thus, this feature could be
132 exploited in the regulation of metabolic pathways in the cells.
133
134 Here, we construct a dynamic switch for autonomous shifting of cells from the
135 biomass mode to the storage lipid synthesis mode by introducing a circuit for a
136 conditional elimination of the glyoxylate cycle, which is the essential bypass for cells
137 growing on acetate, and the key control node in lipid biosynthesis pathway. We
138 demonstrate the functionality of the switch by the improved (both yield and titer)
139 production of wax esters using *A. baylyi* ADP1 as a host.

140 2. Material and Methods

141 Strains and molecular work

142 *A. baylyi ADP1* (DSM 24193, Deutsche Sammlung von Microorganismen und
143 Zellkulturen, Germany) was used in the study. The single gene knock-out strain of *A.*
144 *baylyi* ADP1Δ*aceA*::*tdk*/*Kan*^{r} (ACIAD1084 deleted) was kindly provided by Veronique
145 de Berardinis (Genoscope, France). In the single gene knock-out mutant, the gene in
146 question is replaced with a gene cassette containing a kanamycin resistance gene
147 (Kan^r) (25). For cloning and plasmid amplification, *Escherichia coli* XL1-Blue
148 (Stratagene, USA) was used. The reagents and primers for molecular work were
149 purchased from ThermoFisher Scientific (USA), unless stated otherwise. The primers
150 used in the study are presented in Table 1. The complementation of *aceA* in the knock-
151 out strain was carried out by constructing a gene cassette with the *aceA* gene under
152 an arabinose inducible promoter AraC-pBAD; a previously described gene cassette
153 (16, 26) was used as the scaffold for the construction. The arabinose promoter and

bioRxiv preprint doi: https://doi.org/10.1101/337790; this version posted June 3, 2018. The copyright holder for this preprint (which was not certified by peer review) is the author/funder, who has granted bioRxiv a license to display the preprint in perpetuity. It is made available under aCC-BY 4.0 International license.

154 AraC repressor, designated as ara, were amplified from pBAV1C-ara-LuxCDE plasmid
155 (18) using primers VS10_09 and VS10_10 and inserted to the plasmid iluxAB/pIX (26)
156 using restriction sites MfeI and NdeI. The gene *aceA* (ACIAD1084) was amplified from
157 the genome of ADP1 wt with primers SS17_08 and SS17_09 and cloned to the ara-
158 iluxAB/pIX using restriction sites NdeI and XhoI. Transformations of ADP1 were carried
159 out as described previously (16). The transformed cells were selected on LA plates
160 containing 25 µg/ml chloramphenicol. ADP1 strain with a *poxB* deletion, *A. baylyi*
161 ADP1Δ*poxB*::Cm^r, was used as the reference strain designated as ADP1 wt. All genetic
162 modifications were confirmed with PCR and sequencing.

163 **Cultivations**
164 The components for culture mediums were purchased from Sigma (USA). The strains
165 were cultivated in modified MA/9 minimal salts medium (17) at 25 °C and 300 rpm
166 unless stated otherwise. The medium was supplemented with 25-100 mM Na-acetate
167 or 250 mM glucose, 0.1 % casein amino acids (w/v), and 0-1.0 % L(+)arabinose when
168 appropriate.

169

170 The cultivations for optimizing the arabinose concentration for ADP1-ara-aceA growth
171 were carried out using Tecan Spark® (Tecan, Switzerland) microplate reader in 25 °C
172 for 21 hours with two replicate wells for each strain and arabinose concentration. The
173 medium was supplemented with 25 mM Na-acetate and 0.1 % casein amino acids, and
174 arabinose (concentrations 0; 0.05; 0.1; 0.2; 0.5 or 1.0 %) was used for the induction of
175 *aceA*. Mediums without acetate supplementation was used as the control medium to
176 determine the growth on casein amino acids. The strain ADP1 wt was used as the

bioRxiv preprint doi: https://doi.org/10.1101/337790; this version posted June 3, 2018. The copyright holder for this preprint (which was not certified by peer review) is the author/funder, who has granted bioRxiv a license to display the preprint in perpetuity. It is made available under aCC-BY 4.0 International license.

177 positive control, whereas the knock-out strains ADP1 Δ*aceA*::*Tdk/kan*^{r} and *A. baylyi*
178 ADP1Δ*aceA*::*tdk*/*Kan*^{r} Δ*poxB*::*Cm*^{r} were used as negative controls for growth on
179 acetate. For semi-quantitative determination of the WE production of ADP1-ara-aceA,
180 the cells were cultivated in two parallel 5 ml cultures in the same medium except with
181 50 mM Na-acetate in 5 ml tubes for 30 hours.
182
183 For the quantitative determination of the WEs with NMR, the strain ADP1 wt and
184 ADP1-ara-aceA were cultured in total 600 ml of medium supplemented with 50 mM
185 Na-acetate and 0.5 % (~30 mM) arabinose distributed in 12 Erlenmeyer flasks. HPLC
186 samples were taken every 1-5 hours and two parallel 40 ml samples were taken in five
187 different time-points to quantitatively determine WE (by NMR) and biomass
188 production (as cell dry weight).

189 **Lipid and end-metabolite analyses**
190 The amount of total lipids and WEs were estimated by TLC or quantified by NMR. For
191 TLC, equal volumes of samples (3 ml) from different cultures were taken and the lipids
192 were extracted using 'miniscale' chloroform-methanol extraction as described
193 previously (17). Thirty µl of the chloroform phase was applied on 20 × 10 cm Silica Gel
194 60 F_{254} HPTLC glass plates with 2.5 × 10 cm concentrating zone (Merck, USA). Mobile
195 phase used was n-hexane: diethyl ether: acetic acid 90: 15: 1 and iodine was used for
196 visualization. Jojoba oil was used as the standard for WEs. For comparative evaluation
197 of the intensities of the WE bands on TLC, the Gel analysis method of ImageJ software
198 (rsb.info.nih.gov/ij/index.html) was applied as described in the ImageJ
199 documentation.

bioRxiv preprint doi: https://doi.org/10.1101/337790; this version posted June 3, 2018. The copyright holder for this preprint (which was not certified by peer review) is the author/funder, who has granted bioRxiv a license to display the preprint in perpetuity. It is made available under aCC-BY 4.0 International license.

200

201 For NMR analyses, the 40-ml biomass samples were freeze-dried and the cell dry
202 weight (CDW) was determined gravimetrically. The lipid extraction and the
203 quantitative ^{1}H NMR analysis of WEs was carried out as described earlier (26). The
204 amount of total lipids was determined gravimetrically. The areas of the peaks in the
205 NMR spectrum are directly proportional to the molar concentration of each functional
206 group, yielding specific concentration for WEs in total biomass. The concentration of
207 WEs was calculated from the integrated signal at 4.05 ppm which is characteristic for
208 protons of α-alkoxy-methylene group of esters (–CH2-COO-CH2–). For the calculation
209 of the WE titer in grams per liter, an average molar mass of 506 g/mol was used (17).

210

211 The glucose, acetate, and arabinose concentrations were determined by LC-20AC
212 prominence liquid chromatograph (Shimadzu, USA) equipped with RID-10A refractive
213 index detector, DGU-20A5 prominence degasser, CBM-20A prominence
214 communications bus module, SIL-20AC prominence autosampler, and Shodex SUGAR
215 SH1011 (Showa Denko KK, Japan) as described previously (16).

216 # 3. Results

217 In order to investigate the effect of the knock-out of isocitrate lyase AceA on the
218 growth and WE production in *A. baylyi* ADP1, we employed a knock-out mutant strain
219 *A. baylyi* ADP1 Δ*aceA*::Tdk/kanr (25) for preliminary test cultivations. We observed
220 that when grown on glucose, the cells grow more slowly, but produce WE titers
221 comparable to those of the wild type (wt) strain; after 48 hours of cultivation, the wild
222 type had produced 470±150 mg/l WEs compared to 460±40 mg/l WEs produced by

bioRxiv preprint doi: https://doi.org/10.1101/337790; this version posted June 3, 2018. The copyright holder for this preprint (which was not certified by peer review) is the author/funder, who has granted bioRxiv a license to display the preprint in perpetuity. It is made available under aCC-BY 4.0 International license.

223 the knock-out strain. In opposite to the wt strain, however, the mutant strain did not
224 exhibit growth on minimal medium supplied with acetate as the sole carbon source.
225 This is due to the lack of route for acetyl-CoA to be directed in biosynthetic pathways
226 via malate. Thus, as acetyl-CoA represents the key precursor in both the biomass
227 production through the glyoxylate shunt and the wax ester biosynthesis, we
228 hypothesized that by dynamically regulating the isocitrate lyase, the state of the cells
229 could be switched between biomass and lipid synthesis modes (Fig 1). In order to make
230 the shift dynamic, we introduced an approach for autonomous regulation of the
231 isocitrate lyase AceA; by expressing the enzyme under an arabinose-inducible
232 promoter AraC-pBAD, the induction is gradually repressed due to the depletion of
233 arabinose by the glucose dehydrogenase activity of ADP1. The arabinose inducible
234 promoter has been previously shown to function in *A. baylyi* ADP1 (18, 27). In order
235 to establish a system with maximal linearity and controllability, we constructed a gene
236 cassette for genomic expression of *aceA* (Fig 1c, d). Exploiting the natural
237 transformation machinery of ADP1, the gene cassette was integrated in the genome
238 to replace a gene *poxB* (ACIAD3381), which has been previously shown to be a neutral
239 target site in terms of growth and wax ester production (26, 28). The resulting strain
240 *A. baylyi* ADP1Δ*aceA*::*tdk*/*Kan*^{r} Δ*poxB*::*araC*-pBAD-*aceA*-*Cm*^{r} was designated as ADP1-
241 ara-aceA. The strain *A. baylyi* ADP1Δ*poxB*::*Cm*^{r} was used as the reference strain, from
242 now on designated as the ADP1 wt.
243
244 We investigated the functionality of the complementation in the strain ADP1-ara-aceA
245 in minimal medium supplemented with 50 mM acetate (Figure 2). Arabinose (at

bioRxiv preprint doi: https://doi.org/10.1101/337790; this version posted June 3, 2018. The copyright holder for this preprint (which was not certified by peer review) is the author/funder, who has granted bioRxiv a license to display the preprint in perpetuity. It is made available under aCC-BY 4.0 International license.

246 concentrations 0; 0.1 and 1.0 %) was added to the cultures, and the cultivations were
247 continued for 68 hours. Cells did not grow or consume acetate in the absence of
248 arabinose, indicating sufficiently tight regulation of the arabinose promoter. In the
249 cultures with small amount of arabinose (0.1 %), the cells stopped growing after
250 reaching an optical density (OD) of 0.3 and consumed only 5 mM acetate, whereas
251 with 1.0 % arabinose the cells reached OD ~3.5 along with complete consumption of
252 acetate. The ADP1 wt grew to slightly lower biomass (OD ~2.4) and consumed all the
253 acetate; arabinose supplementation had no effect on the ADP1 wt growth. After 68
254 hours of cultivation, approximately 85 % of the 1% arabinose had been oxidized. The
255 control knockout strains ADP1Δ*aceA::tdk/Kan*^{r} and ADP1*ΔaceA::tdk/Kan*^{r} *ΔpoxB::Cm*^{r}
256 did not exhibit growth nor acetate consumption with or without the presence of
257 arabinose (OD 0 at 0-68 h). We also confirmed, that the AceA expression is repressed
258 due to arabinose oxidation, i.e. the conversion of arabinose to non-inducive form,
259 arabino-lactone and further to arabonate (Figure S1).
260
261 In order to find the optimal arabinose concentration in terms of both biomass and wax
262 ester production, the strain ADP1-ara-aceA was cultivated in several different
263 arabinose concentrations in minimal salts medium supplemented with acetate (Figure
264 3) for 21 hours. ADP1 wt was cultured as the reference strain. Casein amino acids
265 (0.1%) were added to the culture in order to promote the growth and to prevent
266 nitrogen limitation. As indicated by the previous growth experiment, we found that
267 1% arabinose was sufficient to allow the engineered strain to reach the same biomass
268 as ADP1 wt, albeit the cells grew slower. Within the concentration range 0 – 0.2%, only

bioRxiv preprint doi: https://doi.org/10.1101/337790; this version posted June 3, 2018. The copyright holder for this preprint (which was not certified by peer review) is the author/funder, who has granted bioRxiv a license to display the preprint in perpetuity. It is made available under aCC-BY 4.0 International license.

269 small differences in growth pattern or biomass production were observed. The slight
270 increase in OD of uninduced cells is due to the utilization of the casein amino acids
271 present in the growth medium; a same amount of biomass is achieved without acetate
272 supplementation with the wild type strain and the knock-out strain
273 ADP1*ΔaceA::tdk/Kan*^{r}*ΔpoxB::Cm*^{r} with both acetate and casein amino acid
274 supplementation (data not shown). For ADP1 wt, all the growth curves were similar
275 regardless of the arabinose concentration used (data not shown).
276
277 Next, we determined which initial arabinose concentration most optimally distributes
278 the carbon between the biomass and the WE production. The strain ADP1-ara-aceA
279 was cultivated in 5 ml minimal salts medium supplemented with 0.1 % casamino acids
280 and 50 mM acetate with different arabinose concentrations (0; 0.1; 0.2; 0.5% and
281 1.0%) for 30 hours, after which biomass and WE production were determined. A clear
282 correlation between the arabinose concentration and biomass production (OD600)
283 was detected (Figure 4). Without arabinose supplementation, the cells grew to an OD
284 of approximately 0.8, which is due to the utilization of casamino acids (the same OD
285 was obtained with ADP1*ΔaceA::tdk/Kan*^{r}*ΔpoxB::Cm*^{r}). A semi-quantitative lipid
286 analyses based on thin layer chromatography (TLC) was carried out to compare the
287 amount of WEs produced (Figure 5B). For all the cultures, the same sample volume
288 was taken for the analysis, thus representing the titer of WEs produced. Based on
289 image analysis, the intensity of the band representing the wax ester titer increases
290 along with the biomass concentration. However, only a slight difference was observed
291 between the bands of the 0.5% and 1.0% cultures, suggesting that in the culture which

bioRxiv preprint doi: https://doi.org/10.1101/337790; this version posted June 3, 2018. The copyright holder for this preprint (which was not certified by peer review) is the author/funder, who has granted bioRxiv a license to display the preprint in perpetuity. It is made available under aCC-BY 4.0 International license.

292 contains saturating amount of arabinose the growth corresponds to that of the wild-
293 type strain. When the intensities were divided with the optical densities, the highest
294 amounts of WEs (per cell) were produced in the cultures with 0.2% and 0.5%
295 arabinose. Thus, considering both the volumetric titer and the yield of WEs per
296 biomass, the arabinose concentration of 0.5% was found to be optimal in terms of
297 distributing the carbon and cellular resources between biomass and WEs.

298

299 Batch cultivations for ADP1 wt and ADP1-ara-aceA were carried out in minimal
300 medium supplemented with 0.1 % casein amino acids, 50 mM Na-acetate and 0.5 %
301 arabinose. Acetate and arabinose concentrations as well as the WE production (at 5,
302 7, 9 and 10 h time-points) were determined (Figure 5). ADP1 wt consumed all the
303 acetate in approximately 9-10 hours; the amount of biomass increased until the 10-
304 hour time-point, the CDW being 1.3 g/l. The highest amount of WEs was measured at
305 the 9-hour time-point, being 47 mg/g CDW and 60 mg/l. In ADP1 wt, the WEs
306 accounted for 44 % of total lipids. The WE yield was found to be 0.02 g WE/g consumed
307 acetate. The strain ADP1-ara-aceA utilized acetate more steadily and produced less
308 biomass compared to ADP1 wt; the growth ceased after 16 hours along with the
309 arabinose depletion: the biomass remained at 0.6-0.7 g/l CDW between the 16-24
310 hours of cultivation. Thereafter, the WE content of the cells strongly increased, being
311 highest at 38 h time-point, which also increased the amount of total biomass to 1.0
312 g/l. The WE titer was found to be 184 mg/l representing 19 % of CDW, which was 3.8-
313 fold higher compared to the ADP1 wt. In addition, the WEs accounted for 80 % of all

bioRxiv preprint doi: https://doi.org/10.1101/337790; this version posted June 3, 2018. The copyright holder for this preprint (which was not certified by peer review) is the author/funder, who has granted bioRxiv a license to display the preprint in perpetuity. It is made available under aCC-BY 4.0 International license.

314 cellular lipids in ADP1-ara-aceA. The WE yield was 0.08 g WE/g consumed acetate, also
315 being 4-fold higher over the ADP1 wt.

316 4. Discussion

317 Sugars, mainly glucose, have been the major carbon source for the heterotrophic
318 microbial production of fatty acid derived compounds, such as TAGs and WEs, which
319 can be used for the production of biofuels, biochemicals, and other biocommodities
320 (29, 30). However, in order to increase the feasibility and sustainability of the
321 processes, the possibility to utilize alternative carbon sources is of high interest.
322 Organic acids, such as acetate, serves as a low-cost, abundant carbon source for
323 microbial lipid synthesis. Acetate can be readily derived from the hemicellulose
324 fraction of plant biomass or waste streams, or produced from syngases by microbial
325 fermentation (31). For example, we have previously demonstrated the conversion of
326 carbon dioxide to WEs via acetate intermediate by combining microbial
327 electrosynthesis with aerobic lipid synthesis in a two-stage process (32). Many of the
328 potential acetate streams, however, may have dilute acetate concentrations, thus
329 sustaining conditions that are preferable for biomass production rather than for
330 efficient storage carbon synthesis. On the other hand, highly concentrated acetate
331 feeds can inhibit cell growth (33).
332

333 Nitrogen starvation is a commonly used and efficient means to trigger storage lipid
334 accumulation in microbes (34-36). However, in such conditions the cell biomass
335 typically remains low (37), which can result in lower overall product titres. Thus,

bioRxiv preprint doi: https://doi.org/10.1101/337790; this version posted June 3, 2018. The copyright holder for this preprint (which was not certified by peer review) is the author/funder, who has granted bioRxiv a license to display the preprint in perpetuity. It is made available under aCC-BY 4.0 International license.

336 genetic reprogramming would serve as a means to bypass the natural regulation for
337 storage lipid synthesis. Mechanisms behind the regulation in microbes are not well
338 understood, and therefore it has been challenging to genetically drive cells to
339 overproduce the storage compounds or other fatty acid derived products. Previous
340 strategies include for example the manipulation of the conserved carbon storage
341 regulator CsrA through the CsrA-CsrB ribonucleoprotein complex, by which alterations
342 in the central carbon metabolism and fatty acid synthesis regulation have led to
343 favourable changes in both native and non-native product synthesis pathways in *E.*
344 *coli* (38). This approach, however, is rather unspecific and potentially difficult to
345 combine with other (targeted) engineering strategies.

346

347 In this study, we developed an autonomously regulated circuit for programmable
348 synthesis of WEs in a native production host, *A. baylyi* ADP1. The circuit allows the
349 cells to shift from the biomass mode to the WE synthesis mode independent from the
350 carbon/nitrogen ratio or the growth phase of the culture. In practice, we replaced the
351 native isocitrate lyase aceA with an arabinose inducible system, which allows a
352 conditional and timed knockdown of the expression of *aceA*. This enzyme is essential
353 for the biomass production when the cells grow on acetate. The timed repression of
354 aceA expression is achieved by gradually eliminating the inducer, namely arabinose;
355 the native enzyme activity of glucose dehydrogenase Gcd of *A. baylyi* oxidizes
356 arabinose to arabino-lactone and further to arabonate, which in turn cannot serve as
357 inducers. Importantly, and in contrast to other auto-induction-based systems,
358 arabinose oxidation does not interfere with the utilization of the carbon source, here

bioRxiv preprint doi: https://doi.org/10.1101/337790; this version posted June 3, 2018. The copyright holder for this preprint (which was not certified by peer review) is the author/funder, who has granted bioRxiv a license to display the preprint in perpetuity. It is made available under aCC-BY 4.0 International license.

359 acetate, and can be thus considered as an orthogonal system. By adjusting the
360 arabinose concentration, a predefined and optimal amount of biomass can be
361 produced. When the inducer concentration is oxidized below the 'threshold'
362 concentration, the cells shift from the biomass producing mode to the synthesis mode,
363 efficiently directing carbon to product synthesis.
364
365 First, we confirmed that the engineered strain ADP1-ara-aceA with complemented
366 isocitrate lyase was able to grow on acetate as the sole carbon source. We observed
367 that without the presence of arabinose, the cells did not exhibit growth, showing
368 phenotype similar to the knockout strain *A. baylyi* ADP1Δ*aceA*::*tdk*/*Kan*^{r}Δ*poxB*::*Cm*^{r}.
369 We also observed that arabinose concentration 1% is sufficient to allow the growth of
370 ADP1-ara-aceA to reach at least the same biomass as the ADP1 wt.
371
372 Initial arabinose concentrations were in correlation with the obtained biomasses
373 between concentrations 0.2% and 1.0%. The concentration 0.2% was found to be the
374 'threshold' for sufficient biomass production; below this concentration, the cells
375 produced only slightly more biomass compared to the uninduced cells, indicating that
376 arabinose concentrations >0.2% are required for sufficient growth in the studied
377 conditions. This finding was also supported by the reporter induction test; when the
378 cells containing the bacterial luciferase *luxAB* under arabinose promoter were induced
379 with the supernatant from different cultivation time-points (thus having different
380 arabinose concentrations), clear induction of *luxAB* determined as luminescence
381 production was only observed with the sample that contained >0.2% arabinose.

bioRxiv preprint doi: https://doi.org/10.1101/337790; this version posted June 3, 2018. The copyright holder for this preprint (which was not certified by peer review) is the author/funder, who has granted bioRxiv a license to display the preprint in perpetuity. It is made available under aCC-BY 4.0 International license.

382

383 According to the semi-quantitative WE analyses, the cultures supplemented with 0.2%
384 or 0.5% arabinose produced the highest WE yields (per biomass). The cultures that
385 were induced with 1% arabinose produced nearly two times more biomass compared
386 to that of the 0.5% culture but had lower WE yield, indicating that a significant
387 proportion of the carbon was directed to the biomass when 1% arabinose was used.
388 Interestingly, the cultures with little (0.1%) or no arabinose produced the lowest WE
389 yield, suggesting that at least subtle levels of *aceA* expression are required, not only
390 for biomass production but also to support WE synthesis. The WE titres (WEs/volume)
391 of 0.5% and 1.0% cultures were estimated to be very close to each other in the two
392 cultures, whereas 0.2% culture had clearly lower volumetric WE production due to low
393 biomass production. Thus, we considered 0.5% arabinose as the most effective
394 inducer concentration in terms of optimal distribution of carbon between biomass and
395 products.

396

397 For validation of the system, batch cultures for the ADP1 wt and ADP1-ara-aceA were
398 carried out. It was shown that the engineered strain ADP1-ara-aceA efficiently
399 accumulated WEs in simple batch conditions supplied with relatively low substrate
400 concentration (50 mM acetate) and in non-optimal carbon-nitrogen ratio. The strain
401 ADP1-ara-aceA produced 187 mg/l WEs representing 19 % of the CDW and a yield of
402 0.08 g WE/g consumed acetate. As expected, the strain grew more slowly and
403 produced less biomass than ADP1 wt, but the yield of WEs per biomass and per
404 consumed acetate were 3.8 and 4 folds higher compared to ADP1 wt, respectively. In

bioRxiv preprint doi: https://doi.org/10.1101/337790; this version posted June 3, 2018. The copyright holder for this preprint (which was not certified by peer review) is the author/funder, who has granted bioRxiv a license to display the preprint in perpetuity. It is made available under aCC-BY 4.0 International license.

405 addition, the WE titer was found to be 3.1 folds higher compared to that of the ADP1
406 wt. Thus, the dynamic regulation not only improved the yield of WEs per biomass and
407 per used carbon, but clearly excelled the volumetric titer of that of the wild type strain.
408 For comparison, in a previous study (32), *A. baylyi* ADP1 produced WEs from acetate
409 with a titer of approximately 90 mg/l (from higher initial acetate concentration, 100
410 mM), with an average yield of 4 % (carbon/carbon), being equal to 0.02 g WE/g
411 consumed acetate. The highest WE titer reported so far has been 450 mg/l, which was
412 obtained when the key enzyme of the pathway (fatty acyl-CoA reductase) was
413 overexpressed and 5 % glucose was used as the substrate (17). However, the yields
414 (0.04g WE/g glucose and 12.5% WEs of CDW) were lower compared to this study. With
415 external alkane supplementation, up to 17% WEs of CDW has been obtained (39).
416
417 Notably, the amount of WEs per cell was nearly constant in ADP1 wt at the analysed
418 time points, being 3.9-4.3% of the CDW. In ADP1-ara-aceA, by contrast, the amount of
419 WEs per cell strongly increased along with the arabinose depletion; the percentage of
420 WEs per cell increased from 5.2% to 19% between the sampling points. The highest
421 increase in the WE content (from 7.5 to 19%) was achieved after the arabinose
422 concentration reached the 'threshold' 0.2% (equivalent to 15 mM arabinose).
423 Although the shift from biomass mode to lipid mode was rather gradual, the arabinose
424 concentration 0.2% seems to be the key turning point in the cellular state. In the batch
425 culture, initial concentrations 50 mM acetate and 0.5% arabinose were used. By the
426 end of the culture, the arabinose was completely oxidized, and only a small amount
427 (5 mM) of acetate remained unutilized. Thus, by adjusting the substrate and inducer

bioRxiv preprint doi: https://doi.org/10.1101/337790; this version posted June 3, 2018. The copyright holder for this preprint (which was not certified by peer review) is the author/funder, who has granted bioRxiv a license to display the preprint in perpetuity. It is made available under aCC-BY 4.0 International license.

428 concentrations, the system is potentially scalable to a wide range of substrate
429 concentrations. Moreover, coupling this system with other engineering strategies,
430 such as introducing additional knock-outs (16) and/or overexpression of key enzymes
431 of the pathway (17) could further improve the WE production.
432
433 Considering not only the efficient redirection of carbon to product, but also the
434 downstream processing, the purity of the product is important. In ADP1-ara-aceA,
435 WEs constituted 80% of total lipids, indicating high purity of the desired product. In
436 ADP1 wt, only 44% of the total lipids were WEs.
437
438 The results from different experiments indicate that at least low levels of isocitrate
439 lyase are required to maintain WE production from acetate, potentially due to the
440 requirements for cells to generate e.g. NADPH for the synthesis. This hypothesis was
441 also supported by a further observation in an additional experimental set-up where
442 the WE content of the *aceA* knockout strain did not increase after a transfer from a
443 glucose medium to an acetate medium (data not shown). While arabinose
444 concentration <0.2% is not sufficient to promote biomass production, it allows the
445 cells to synthetize and maintain the required cofactor balance, and to efficiently
446 produce WEs.
447
448 Rapid advancements in the CRISPR/Cas9 technologies have broaden the tools
449 available for targeted genome engineering, and especially the employment of the
450 deactivated Cas9 (dCas9) has recently gained interest in the context of targeted gene

bioRxiv preprint doi: https://doi.org/10.1101/337790; this version posted June 3, 2018. The copyright holder for this preprint (which was not certified by peer review) is the author/funder, who has granted bioRxiv a license to display the preprint in perpetuity. It is made available under aCC-BY 4.0 International license.

451 silencing (40, 41). While the dCas9 –based tools have been shown to be functional and
452 applicable in a wide range of (microbial) hosts, challenges related to unpredictability,
453 cellular burden and off-targeting may limit its use (42, 43). In addition, at least two
454 different constructs are typically required for the fine-tuned expression of dCas9 and
455 the RNA elements, and the system cannot be easily operated 'hands-free' without a
456 timed addition of an inducer. In this context, the system described here provides a
457 straight-forward, readily controllable, and reliable set-up for conditional and timed
458 gene knock-down. In addition, other interesting synthetic biology hosts such as *P.*
459 *putida* (44, 45) exhibit the same glucose dehydrogenase activity and could thus find
460 this strategy applicable. However, the transferability of this system to others hosts
461 such as *E. coli* and *S. cerevisiae* remains to be investigated in the future.
462
463 Our system serves as a simple and scalable method for dynamic, 'hands-free'
464 regulation of growth-essential reactions in the cell, which allows targeted and
465 adjusted biomass and product synthesis. Here, the dynamic regulation system was
466 exploited in the conversion of acetate to carbon-rich storage compounds, namely wax
467 esters, that are otherwise not efficiently accumulated in cells without optimized
468 conditions and high carbon-nitrogen ratio. Moreover, the system could be potentially
469 utilized and generalized for a broad range of synthesis pathways that are dependent
470 on acetyl-CoA (17, 46). In addition, other sustainable carbon sources, such as lignin-
471 derived compounds (47-49) would be compatible with this system.

bioRxiv preprint doi: https://doi.org/10.1101/337790; this version posted June 3, 2018. The copyright holder for this preprint (which was not certified by peer review) is the author/funder, who has granted bioRxiv a license to display the preprint in perpetuity. It is made available under aCC-BY 4.0 International license.

472 ## 5. Conclusions

473 We showed that an autonomously regulated genetic switch allowed the dynamic
474 decoupling of biomass and wax ester production in engineered *A. baylyi* ADP1, which
475 resulted in 3-4 fold improvements in the wax ester yield and titer compared to the
476 wild type strain. Shifting the cells from a biomass mode to a product synthesis mode
477 was achieved by gradually repressing the growth essential gene *aceA* by a simple and
478 robust set-up. The engineered strain produced 19% WEs of its cell dry weight, being
479 the highest reported among microbes. The study demonstrates the possibility to
480 bypass the challenges related to highly regulated storage lipid synthesis, and
481 strengthens the status of *A. baylyi* ADP1 as a convenient host for metabolic
482 engineering and high-value lipid production from sustainable substrates.

483 ## Acknowledgements

484 Funding: This work was supported by the Academy of Finland (grant numbers 286450,
485 310135, 310188, and 311986).

486 ## References

487 1. Tan SZ & Prather KL (2017) Dynamic pathway regulation: recent advances and
488 methods of construction. *Curr Opin Chem Biol* 41:28-35.
489
490 2. Soma Y, Tsuruno K, Wada M, Yokota A, & Hanai T (2014) Metabolic flux
491 redirection from a central metabolic pathway toward a synthetic pathway using
492 a metabolic toggle switch. *Metabolic engineering* 23:175-184.

bioRxiv preprint doi: https://doi.org/10.1101/337790; this version posted June 3, 2018. The copyright holder for this preprint (which was not certified by peer review) is the author/funder, who has granted bioRxiv a license to display the preprint in perpetuity. It is made available under aCC-BY 4.0 International license.

493

494 3. Soma Y & Hanai T (2015) Self-induced metabolic state switching by a tunable
495 cell density sensor for microbial isopropanol production. *Metabolic engineering*
496 30:7-15.

497

498 4. Solomon KV, Sanders TM, & Prather KL (2012) A dynamic metabolite valve for
499 the control of central carbon metabolism. *Metabolic engineering* 14(6):661-671.

500

501 5. Brockman IM & Prather KL (2015) Dynamic knockdown of E. coli central
502 metabolism for redirecting fluxes of primary metabolites. *Metabolic engineering*
503 28:104-113.

504

505 6. Moser F*, et al.* (2012) Genetic circuit performance under conditions relevant for
506 industrial bioreactors. *ACS Synthetic Biology* 1(11):555-564.

507

508 7. Wältermann M*, et al.* (2005) Mechanism of lipid-body formation in prokaryotes:
509 how bacteria fatten up. *Molecular microbiology* 55(3):750-763.

510

511 8. Wältermann M & Steinbüchel A (2005) Neutral lipid bodies in prokaryotes:
512 recent insights into structure, formation, and relationship to eukaryotic lipid
513 depots. *Journal of bacteriology* 187(11):3607-3619.

514

bioRxiv preprint doi: https://doi.org/10.1101/337790; this version posted June 3, 2018. The copyright holder for this preprint (which was not certified by peer review) is the author/funder, who has granted bioRxiv a license to display the preprint in perpetuity. It is made available under aCC-BY 4.0 International license.

515 9. Xu P, Li L, Zhang F, Stephanopoulos G, & Koffas M (2014) Improving fatty
516 acids production by engineering dynamic pathway regulation and metabolic
517 control. *Proceedings of the National Academy of Sciences of the United States*
518 *of America* 111(31):11299-11304.

519

520 10. Teixeira PG, Ferreira R, Zhou YJ, Siewers V, & Nielsen J (2017) Dynamic
521 regulation of fatty acid pools for improved production of fatty alcohols in
522 Saccharomyces cerevisiae. *Microbial Cell Factories* 16(1):45.

523

524 11. Kurosawa K, Boccazzi P, de Almeida NM, & Sinskey AJ (2010) High-cell-
525 density batch fermentation of Rhodococcus opacus PD630 using a high
526 glucose concentration for triacylglycerol production. *J Biotechnol* 147(3-4):212-
527 218.

528

529 12. Xu J, Liu N, Qiao K, Vogg S, & Stephanopoulos G (2017) Application of
530 metabolic controls for the maximization of lipid production in semicontinuous
531 fermentation. *Proceedings of the National Academy of Sciences of the United*
532 *States of America* 114(27):E5308-E5316.

533

534 13. Runguphan W & Keasling JD (2014) Metabolic engineering of Saccharomyces
535 cerevisiae for production of fatty acid-derived biofuels and chemicals.
536 *Metabolic engineering* 21:103-113.

537

bioRxiv preprint doi: https://doi.org/10.1101/337790; this version posted June 3, 2018. The copyright holder for this preprint (which was not certified by peer review) is the author/funder, who has granted bioRxiv a license to display the preprint in perpetuity. It is made available under aCC-BY 4.0 International license.

538 14. Plassmeier J, Li Y, Rueckert C, & Sinskey AJ (2016) Metabolic engineering
539 Corynebacterium glutamicum to produce triacylglycerols. *Metabolic*
540 *engineering* 33:86-97.

541

542 15. Tai M & Stephanopoulos G (2013) Engineering the push and pull of lipid
543 biosynthesis in oleaginous yeast Yarrowia lipolytica for biofuel production.
544 *Metabolic engineering* 15:1-9.

545

546 16. Santala S*, et al.* (2011) Improved triacylglycerol production in *Acinetobacter*
547 *baylyi* ADP1 by metabolic engineering. *Microb Cell Fact* 10:36.

548

549 17. Lehtinen T, Efimova E, Santala S, & Santala V (2018) Improved fatty aldehyde
550 and wax ester production by overexpression of fatty acyl-CoA reductases.
551 *Microbial Cell Factories* 17(1):19.

552

553 18. Santala S, Efimova E, Koskinen P, Karp MT, & Santala V (2014) Rewiring the
554 wax ester production pathway of *Acinetobacter baylyi* ADP1. *ACS Synth Biol*
555 3(3):145-151.

556

557 19. Klinke S, Dauner M, Scott G, Kessler B, & Witholt B (2000) Inactivation of
558 isocitrate lyase leads to increased production of medium-chain-length poly(3-
559 hydroxyalkanoates) in Pseudomonas putida. *Applied and environmental*
560 *microbiology* 66(3):909-913.

561

bioRxiv preprint doi: https://doi.org/10.1101/337790; this version posted June 3, 2018. The copyright holder for this preprint (which was not certified by peer review) is the author/funder, who has granted bioRxiv a license to display the preprint in perpetuity. It is made available under aCC-BY 4.0 International license.

562 20. Young DM, Parke D, & Ornston LN (2005) Opportunities for genetic
563 investigation afforded by Acinetobacter baylyi, a nutritionally versatile bacterial
564 species that is highly competent for natural transformation. *Annual review of*
565 *microbiology* 59:519-551.

566

567 21. Kannisto M, Aho T, Karp M, & Santala V (2014) Metabolic engineering of
568 Acinetobacter baylyi ADP1 for improved growth on gluconate and glucose.
569 *Applied and environmental microbiology* 80(22):7021-7027.

570

571 22. Kannisto MS*, et al.* (2015) Metabolic engineering of Acinetobacter baylyi ADP1
572 for removal of Clostridium butyricum growth inhibitors produced from
573 lignocellulosic hydrolysates. *Biotechnol Biofuels* 8(1):1-10.

574

575 23. Carr EL, Kampfer P, Patel BK, Gurtler V, & Seviour RJ (2003) Seven novel
576 species of Acinetobacter isolated from activated sludge. *International journal of*
577 *systematic and evolutionary microbiology* 53(Pt 4):953-963.

578

579 24. Barbe V*, et al.* (2004) Unique features revealed by the genome sequence of
580 Acinetobacter sp. ADP1, a versatile and naturally transformation competent
581 bacterium. *Nucleic acids research* 32(19):5766-5779.

582

583 25. de Berardinis V*, et al.* (2008) A complete collection of single-gene deletion
584 mutants of *Acinetobacter baylyi* ADP1. *Molecular systems biology* 4:174.

585

bioRxiv preprint doi: https://doi.org/10.1101/337790; this version posted June 3, 2018. The copyright holder for this preprint (which was not certified by peer review) is the author/funder, who has granted bioRxiv a license to display the preprint in perpetuity. It is made available under aCC-BY 4.0 International license.

586 26. Santala S, Efimova E, Karp M, & Santala V (2011) Real-time monitoring of
587 intracellular wax ester metabolism. *Microb Cell Fact* 10:75.
588
589 27. Murin CD, Segal K, Bryksin A, & Matsumura I (2012) Expression vectors for
590 *Acinetobacter baylyi* ADP1. *Applied and environmental microbiology*
591 78(1):280-283.
592
593 28. Santala V, Karp M, & Santala S (2016) Bioluminescence based system for
594 rapid detection of natural transformation. *FEMS microbiology letters*.
595
596 29. Lennen RM & Pfleger BF (2013) Microbial production of fatty acid-derived fuels
597 and chemicals. *Current opinion in biotechnology* 24(6):1044-1053.
598
599 30. Marella ER, Holkenbrink C, Siewers V, & Borodina I (2018) Engineering
600 microbial fatty acid metabolism for biofuels and biochemicals. *Current opinion*
601 *in biotechnology* 50:39-46.
602
603 31. Bengelsdorf FR, Straub M, & Durre P (2013) Bacterial synthesis gas (syngas)
604 fermentation. *Environ Technol* 34(13-16):1639-1651.
605
606 32. Lehtinen T, *et al.* (2017) Production of long chain alkyl esters from carbon
607 dioxide and electricity by a two-stage bacterial process. *Bioresource*
608 *Technology* 243:30-36.

bioRxiv preprint doi: https://doi.org/10.1101/337790; this version posted June 3, 2018. The copyright holder for this preprint (which was not certified by peer review) is the author/funder, who has granted bioRxiv a license to display the preprint in perpetuity. It is made available under aCC-BY 4.0 International license.

609

610 33. Trček J, Mira NP, & Jarboe LR (2015) Adaptation and tolerance of bacteria
611 against acetic acid. *Applied microbiology and biotechnology* 99(15):6215-6229.

612

613 34. Breuer G, Lamers PP, Martens DE, Draaisma RB, & Wijffels RH (2012) The
614 impact of nitrogen starvation on the dynamics of triacylglycerol accumulation in
615 nine microalgae strains. *Bioresource Technology* 124:217-226.

616

617 35. Alvarez HM & Steinbüchel A (2002) Triacylglycerols in prokaryotic
618 microorganisms. *Applied microbiology and biotechnology* 60(4):367-376.

619

620 36. Ishige T, Tani A, Sakai Y, & Kato N (2003) Wax ester production by bacteria.
621 *Current opinion in microbiology* 6(3):244-250.

622

623 37. Amara S, *et al.* (2016) Characterization of key triacylglycerol biosynthesis
624 processes in rhodococci. *Sci Rep* 6:24985.

625

626 38. McKee AE, *et al.* (2012) Manipulation of the carbon storage regulator system
627 for metabolite remodeling and biofuel production in Escherichia coli. *Microbial*
628 *Cell Factories* 11:79.

629

bioRxiv preprint doi: https://doi.org/10.1101/337790; this version posted June 3, 2018. The copyright holder for this preprint (which was not certified by peer review) is the author/funder, who has granted bioRxiv a license to display the preprint in perpetuity. It is made available under aCC-BY 4.0 International license.

630 39. Ishige T, *et al.* (2002) Wax ester production from n-alkanes by Acinetobacter
631 sp. strain M-1: ultrastructure of cellular inclusions and role of acyl coenzyme A
632 reductase. *Applied and environmental microbiology* 68(3):1192-1195.
633
634 40. Larson MH, *et al.* (2013) CRISPR interference (CRISPRi) for sequence-specific
635 control of gene expression. *Nat Protoc* 8(11):2180-2196.
636
637 41. Peters JM, *et al.* (2016) A Comprehensive, CRISPR-based Functional Analysis
638 of Essential Genes in Bacteria. *Cell* 165(6):1493-1506.
639
640 42. Nielsen AA & Voigt CA (2014) Multi-input CRISPR/Cas genetic circuits that
641 interface host regulatory networks. *Molecular systems biology* 10:763.
642
643 43. Cui L, *et al.* (2018) A CRISPRi screen in E. coli reveals sequence-specific
644 toxicity of dCas9. *Nat Commun* 9(1):1912.
645
646 44. Nikel PI & de Lorenzo V (2018) Pseudomonas putida as a functional chassis
647 for industrial biocatalysis: From native biochemistry to trans-metabolism.
648 *Metabolic engineering*.
649
650 45. Nikel PI, Chavarria M, Danchin A, & de Lorenzo V (2016) From dirt to industrial
651 applications: Pseudomonas putida as a Synthetic Biology chassis for hosting
652 harsh biochemical reactions. *Curr Opin Chem Biol* 34:20-29.

bioRxiv preprint doi: https://doi.org/10.1101/337790; this version posted June 3, 2018. The copyright holder for this preprint (which was not certified by peer review) is the author/funder, who has granted bioRxiv a license to display the preprint in perpetuity. It is made available under aCC-BY 4.0 International license.

653

654 46. Lehtinen T, Santala V, & Santala S (2017) Twin-layer biosensor for real-time
655 monitoring of alkane metabolism. *FEMS microbiology letters* 364(6).

656

657 47. Linger JG*, et al.* (2014) Lignin valorization through integrated biological
658 funneling and chemical catalysis. *Proceedings of the National Academy of*
659 *Sciences of the United States of America* 111(33):12013-12018.

660

661 48. Salvachúa D, Karp EM, Nimlos CT, Vardon DR, & Beckham GT (2015)
662 Towards lignin consolidated bioprocessing: simultaneous lignin
663 depolymerization and product generation by bacteria. *Green Chemistry* DOI:
664 10.1039/c5gc01165e.

665

666 49. Salmela MM*, et al.* (2018) Molecular tools for selective recovery and detection
667 of lignin-derived molecules. *Green Chemistry*.

668

669

670

671

bioRxiv preprint doi: https://doi.org/10.1101/337790; this version posted June 3, 2018. The copyright holder for this preprint (which was not certified by peer review) is the author/funder, who has granted bioRxiv a license to display the preprint in perpetuity. It is made available under aCC-BY 4.0 International license.

672 # Figure legends
673

674 **Figure 1.** An autonomously regulated switch for shifting the cells from a biomass to a
675 product synthesis mode. A) Wax ester synthesis strongly competes with biomass
676 production; In the wild type cells, efficient wax ester synthesis is triggered only in
677 defined conditions (i.e. in conditions with nitrogen starvation and excess carbon). In
678 normal growth conditions, most of the carbon is directed to biomass production and
679 cell maintenance. B) The ADP1 wild type strain utilizes acetate for biomass production
680 through a glyoxylate shunt in citric acid cycle. Isocitrate lyase (AceA) is the key enzyme
681 in the glyoxylate shunt and thus essential for growth on acetate. Strain lacking this
682 enzyme is unable to grow on acetate as the sole carbon source. C) The genetic
683 construct for dynamic regulation of *aceA* expression and growth. In the construct,
684 *aceA* is placed under the arabinose-inducible promoter AraC-pBAD. When cultured on
685 acetate, the arabinose used as the inducer is slowly oxidized by the native glucose
686 dehydrogenase Gcd of ADP1, gradually repressing the expression of AceA. Arabinose
687 oxidation does not serve as the carbon source or interfere with the acetate utilization,
688 thus being orthogonal to the circuit function. D) Along with the inducer depletion
689 (arabinose oxidation), the cells gradually shift from the biomass mode to the lipid
690 synthesis mode; the less there is arabinose left in the culture, a higher proportion of
691 the carbon flux is directed to the product. The amount of biomass can be simply
692 regulated by adjusting the initial arabinose concentration.
693

bioRxiv preprint doi: https://doi.org/10.1101/337790; this version posted June 3, 2018. The copyright holder for this preprint (which was not certified by peer review) is the author/funder, who has granted bioRxiv a license to display the preprint in perpetuity. It is made available under aCC-BY 4.0 International license.

694 **Figure 2.** Growth of ADP1 wt and the engineered strain ADP1-ara-aceA in minimal
695 medium. The cells were cultured for 68 hours at 25 °C in MSM supplemented with 50
696 mM Na-acetate as the sole carbon source. Arabinose concentrations of 0; 0.1 and 1.0%
697 (for ADP1 wt 0 and 1%) were used for the induction. Optical densities representing
698 biomasses are presented as an average of two individual replicates.
699
700 **Figure 3.** Growth of ADP1-ara-aceA and ADP1 wt with different arabinose
701 concentrations. The cells were cultured in MA/9 medium supplemented with 25 mM
702 acetate, 0.1% cas.amino acids, and arabinose (0-1%) at 25 °C in micro well-plates for
703 21 hours. The optical densities are presented as the average of three different
704 replicate wells. For ADP1 wt, only the growth curve of the culture containing 1%
705 arabinose is shown.
706
707 **Figure 4.** Biomass and wax ester production by ADP1-ara-aceA induced with different
708 arabinose concentrations. ADP1-ara-aceA was cultured in MA/9 supplemented with
709 50 mM acetate, 0.1% casam, and arabinose (0, 0.1, 0.2, 0.5, or 1.0%) for 30 hours. A)
710 The amount of the produced biomass (at the end-point) was determined by optical
711 density (600 nm) measurement, presented as an average of two individual replica
712 cultures. B) Wax ester production in the cultures with different arabinose
713 concentrations were determined by thin layer chromatography analysis, for which 3
714 ml samples for taken from each culture. Jojoba oil was used as the standard.
715

bioRxiv preprint doi: https://doi.org/10.1101/337790; this version posted June 3, 2018. The copyright holder for this preprint (which was not certified by peer review) is the author/funder, who has granted bioRxiv a license to display the preprint in perpetuity. It is made available under aCC-BY 4.0 International license.

716 **Figure 5.** Acetate utilization, arabinose oxidation, and the accumulation of wax esters
717 (WE) in the batch cultures of A) ADP1 wt and B) ADP1-ara-aceA. The cells were
718 cultivated in MA/9 medium supplemented with 50 mM acetate, 0.1% cas. amino acids,
719 and 0.5% arabinose for 12 h (ADP1 wt) or 38 h (ADP1-ara-aceA). For the arabinose and
720 acetate concentrations determined by HPLC, the average and standard deviation for
721 samples from two individual cultures are presented. Similarly, the WEs were
722 quantitatively analyzed by NMR from two individual cultures. The WE production at
723 different time-points is presented as mg/g CDW to demonstrate the different
724 accumulation patterns of the strains.

725
726

bioRxiv preprint doi: https://doi.org/10.1101/337790; this version posted June 3, 2018. The copyright holder for this preprint (which was not certified by peer review) is the author/funder, who has granted bioRxiv a license to display the preprint in perpetuity. It is made available under aCC-BY 4.0 International license.

727 # Tables

728

729 **Table 1.** List of primers used in the study.

730

Name	*Sequence (5'-> 3')*
VS10_9	CAATGAATTCCGATAAAAGCGGATTCCTGAC
VS10_10	ATCCCATATGTAATTCCTCCTGTTAG
SS17_08	AATACATATGACATATCAATCAGCTCTTGAGC
SS17_09	TAATACAATTGCGAACAGGCTTATGTCAAGACGTC

731

732

733

734

735

736

bioRxiv preprint doi: https://doi.org/10.1101/337790; this version posted June 3, 2018. The copyright holder for this preprint (which was not certified by peer review) is the author/funder, who has granted bioRxiv a license to display the preprint in perpetuity. It is made available under aCC-BY 4.0 International license.

737
738

739 Figure 1.

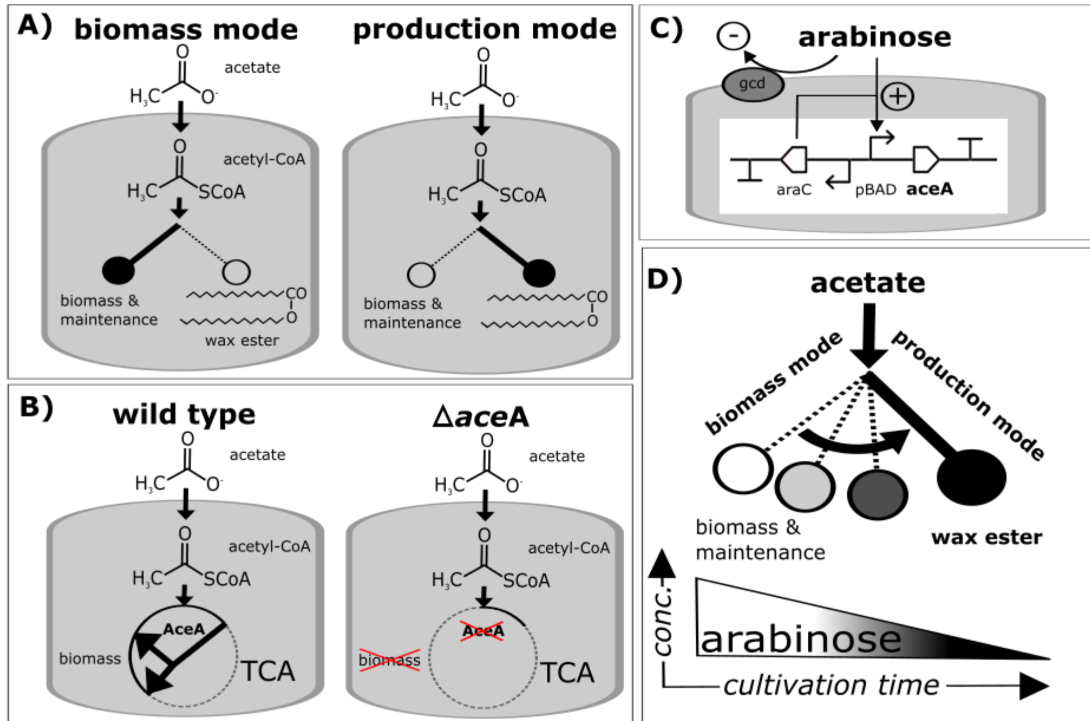

740

741

bioRxiv preprint doi: https://doi.org/10.1101/337790; this version posted June 3, 2018. The copyright holder for this preprint (which was not certified by peer review) is the author/funder, who has granted bioRxiv a license to display the preprint in perpetuity. It is made available under aCC-BY 4.0 International license.

742 Figure 2.

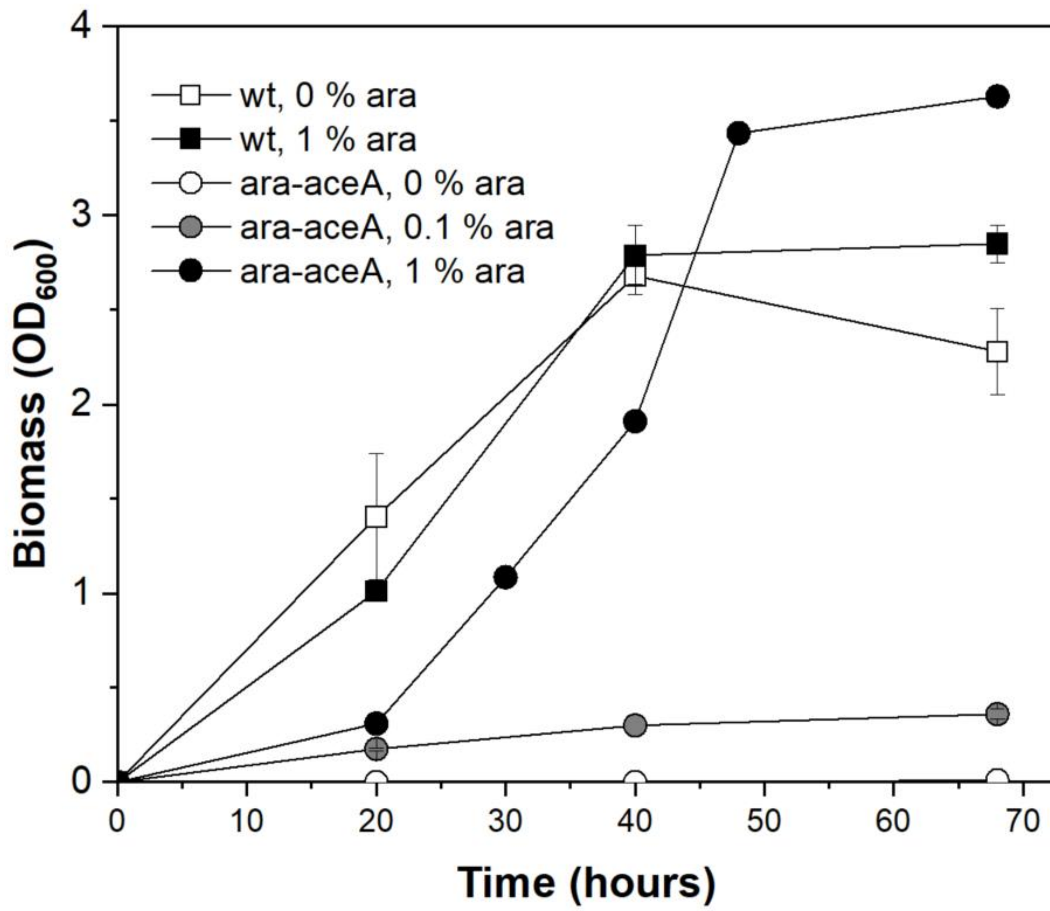

743

744

bioRxiv preprint doi: https://doi.org/10.1101/337790; this version posted June 3, 2018. The copyright holder for this preprint (which was not certified by peer review) is the author/funder, who has granted bioRxiv a license to display the preprint in perpetuity. It is made available under aCC-BY 4.0 International license.

745 Figure 3.

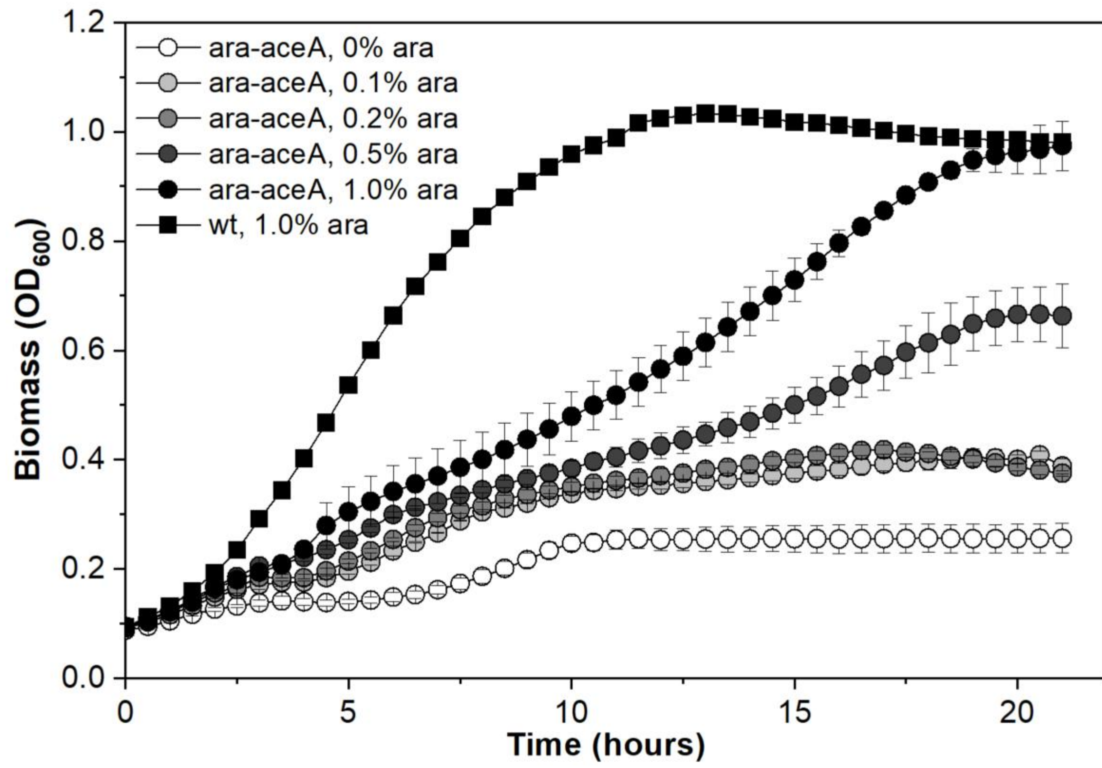

746

747

748

bioRxiv preprint doi: https://doi.org/10.1101/337790; this version posted June 3, 2018. The copyright holder for this preprint (which was not certified by peer review) is the author/funder, who has granted bioRxiv a license to display the preprint in perpetuity. It is made available under aCC-BY 4.0 International license.

749 Figure 4
750

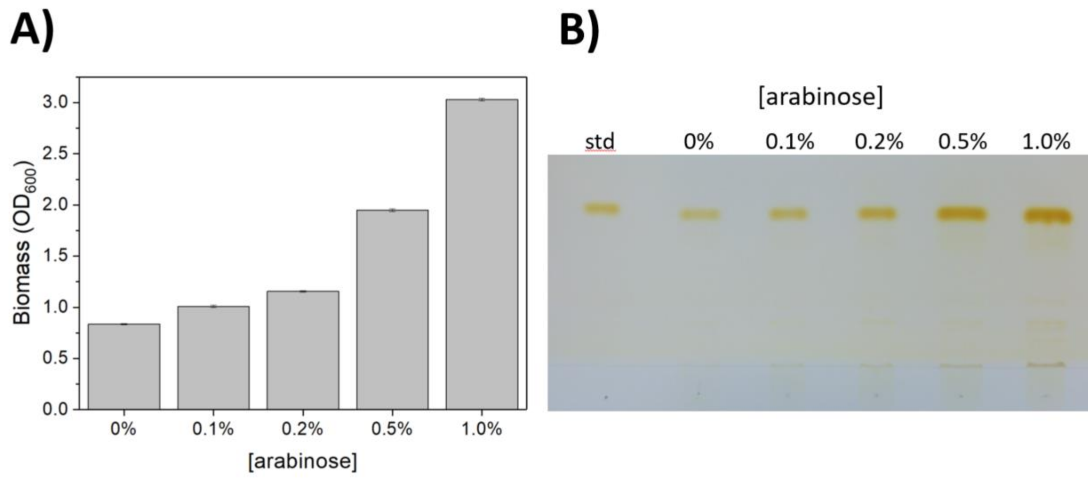

751
752
753

bioRxiv preprint doi: https://doi.org/10.1101/337790; this version posted June 3, 2018. The copyright holder for this preprint (which was not certified by peer review) is the author/funder, who has granted bioRxiv a license to display the preprint in perpetuity. It is made available under aCC-BY 4.0 International license.

754 Figure 5A.

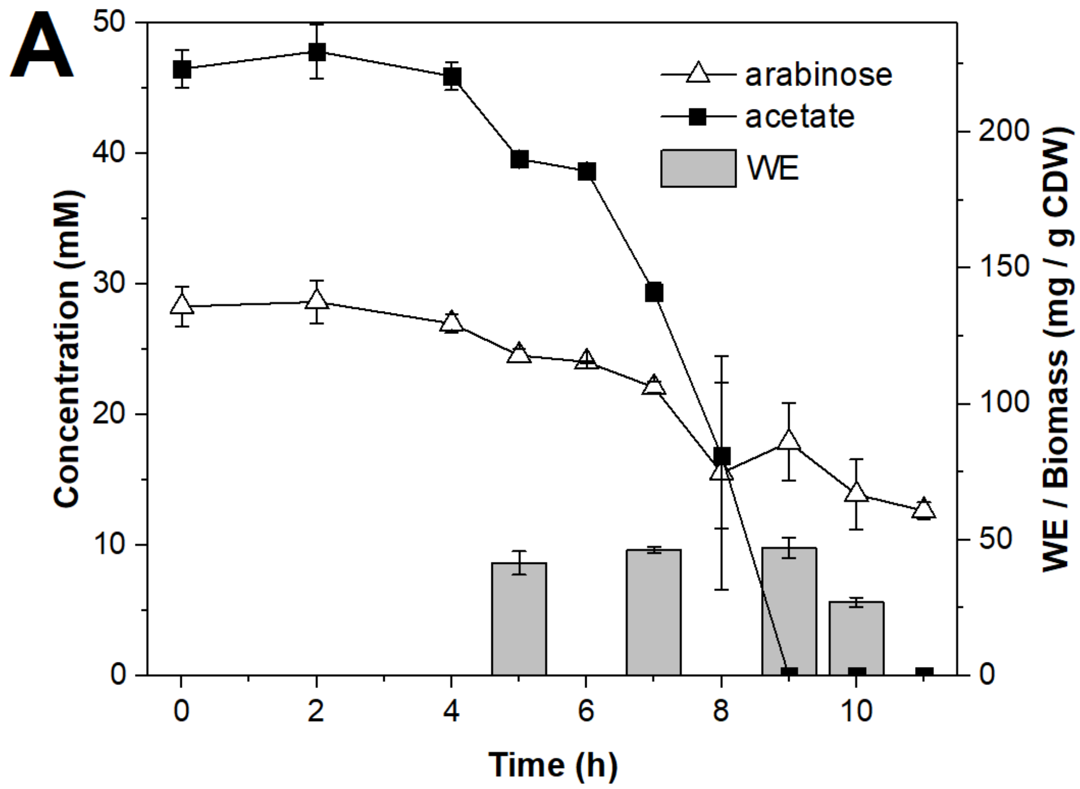

755

756

bioRxiv preprint doi: https://doi.org/10.1101/337790; this version posted June 3, 2018. The copyright holder for this preprint (which was not certified by peer review) is the author/funder, who has granted bioRxiv a license to display the preprint in perpetuity. It is made available under aCC-BY 4.0 International license.

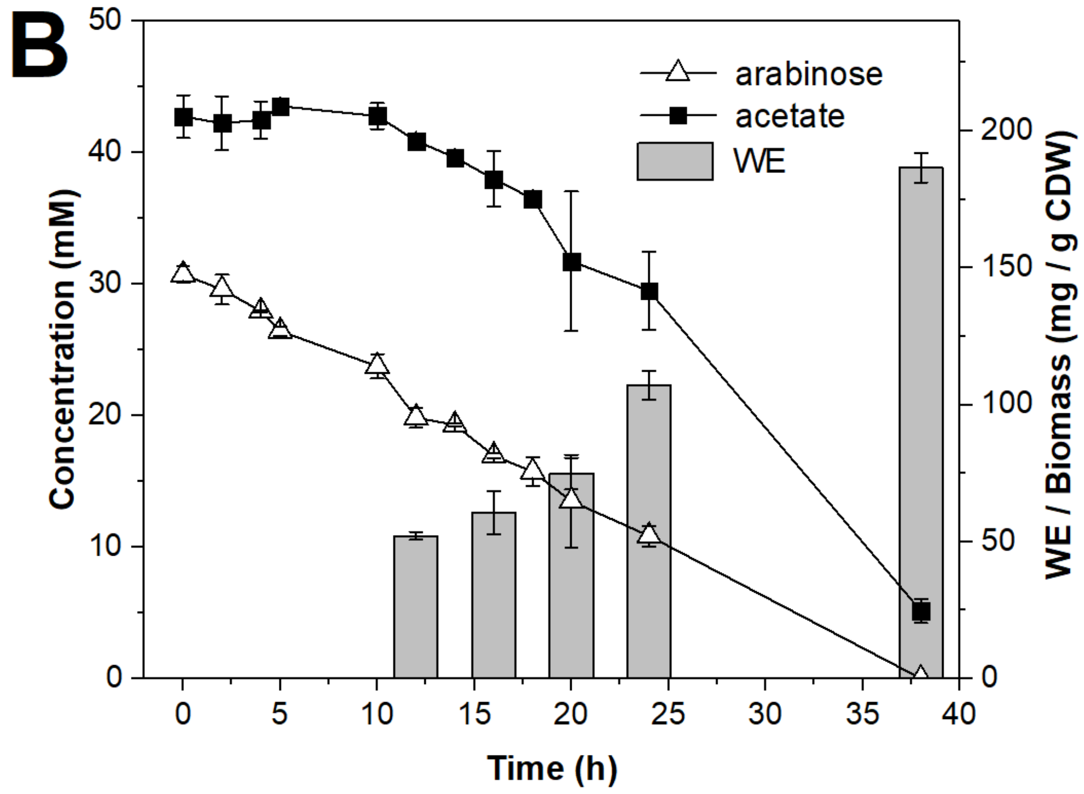

757
758
759